Geol. Mag. **148** (*1*), *2011, pp. 171–182.* © *Cambridge University Press 2010*
doi:10.1017/S0016756810000610

Geometrical similarity in successively developed folds and sheath folds in the basement rocks of the northwestern Indian Shield

DEEPAK C. SRIVASTAVA*

Department of Earth Sciences, I. I. T. Roorkee, Roorkee-247667 (Uttarakhand), India

(*Received* 27 October 2009; *accepted* 3 June 2010; *first published online* 20 August 2010)

Abstract – An intensely deformed gneiss–migmatite terrane and a relatively undeformed granulite–granitoid terrane constitute the bulk of Precambrian basement in the northwestern Indian Shield. This article traces the structural evolution in the gneiss–migmatite terrane, where traditional methods of structural analysis are difficult to apply, and shows how successively developed folds can assume identical geometry and orientation at an advanced stage of progressive ductile shearing. The gneiss–migmatite terrane exemplifies a regional-scale ductile shear zone that preserves the history of polyphase folding and sheath folding. Geometrical similarity between individual/domain-scale sheath folds and mesoscopic/regional-scale folds implies that sheath folding is common at all scales in the gneiss–migmatite terrane. As the mylonite foliation that traces successive folds is curviplanar, the successively initiated hinge lines were curvilinear from their inception in the shear zone. At the advanced stage of ductile shearing, the hinge line curvatures were accentuated due to their rotation towards subvertically directed maximum stretching (*X*), and variably oriented fold axial planes were brought into approximate parallelism with the upright principal plane (*XY*) of the bulk strain ellipsoid. Eventually all the folds, irrespective of their relative order of development, became strongly non-cylindrical, extremely tight, isoclinal and approximately co-planar with respect to each other. It is due to the above geometrical modifications during ductile shearing that folds, irrespective of their order of development, now appear identical with respect to isoclinal geometry, axial plane orientation and hinge line curvilinearity. Evidence from the fold orientations, the deformed lineation patterns and the sheath fold geometry suggest that the shearing occurred in a general shear type of bulk strain, and NNW–SSE-directed subhorizontal compression resulted in subvertically directed stretching in the gneiss–migmatite terrane.

Keywords: ductile shear zones, interference pattern, sheath folds, deformed lineations, mylonite.

1. Introduction

Structural geologists have long documented folds, refolded folds and sheath folds in ductile shear zones (Carreras, Estrada & White, 1977; Rhodes & Gayer, 1977; Minnigh, 1979; Henderson, 1981; Lacassin & Mattauer, 1985; Faure, 1985; Ghosh & Sengupta, 1987; Holdsworth, 1990; Goscombe, 1991; Mukhopadhayay *et al.* 1997; Searle & Alsop, 2007; Alsop & Carreras, 2007; Alsop, Holdsworth & McCaffrey, 2007). These studies have been complemented by several experimental and numerical simulations that provide an insight into the mechanism of refolding and sheath folding in shear zones (Quinquis *et al.* 1978; Cobbold & Quinquis, 1980; Platt, 1983; Alsop & Holdsworth, 2006; Marques, Guerreiro & Fernandes, 2008).

There are, however, only a few studies on the systematic structural analysis of large-scale ductile shear zones that preserve the history of polyphase folding and successive sheath folding (Goscombe, 1991; Mawer & Williams, 1991; Mies, 1993; Ghosh, Hazra & Sengupta, 1999; Alsop & Holdsworth, 1999, 2004*a*,*b*, 2007; Fowler & Kalioubi, 2002; Searle & Alsop, 2007). A limitation in structural analysis in large-scale shear zones is the difficulty in dividing the shear zones into spatial domains of cylindrical folding (Turner & Weiss, 1963; Ramsay & Huber, 1987); the folds in shear zones are commonly non-cylindrical down to centimetre-scale because of sheath folding. This article provides a detailed structural analysis of a large-scale shear zone, where folds are non-cylindrical from a centimetre- to kilometre-scale, and shows how successively developed folds can assume an approximately identical style during the course of progressive ductile shearing.

*E-mail: dpkesfes@iitr.ernet.in

2. Geological setting

The northwestern Indian Shield comprises a gneiss–migmatite–granulite basement and the cover rocks that consist of volcano-sedimentary sequences and the carbonate sequences of the Aravalli and Delhi supergroups, and the Raialo Group, respectively (Heron, 1953; Sinha-Roy, Malhotra & Mohanty, 1998). The basement, namely the Banded Gneissic Complex, is mainly exposed in two sectors in the state of Rajasthan: (1) the southern sector to the east and southeast of Udaipur, and (2) the northern sector to the east of Masuda (Fig. 1). Structural complexities in the southern sector have been studied extensively and explained in terms of superposed folding over the last three decades by Naha and his associates (Naha & Mohanty, 1990; and references therein) and

https://doi.org/10.1017/S0016756810000610 Published online by Cambridge University Press

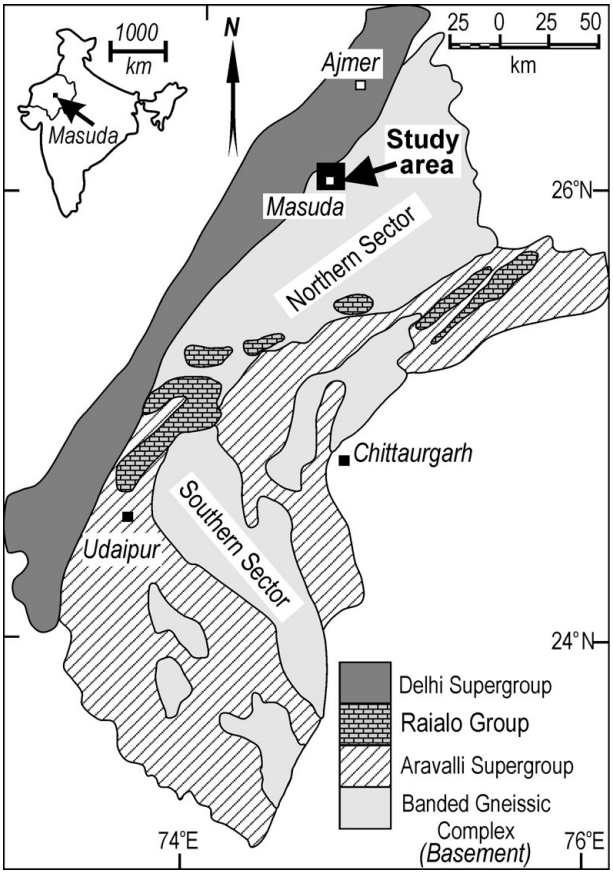

Figure 1. Geological setting of Precambrian terrane in northwestern Indian Shield (after Heron, 1953). The basement consists of Banded Gneissic Complex, and the cover sequences comprise Aravalli Supergroup, Raialo Group and Delhi Supergroup rocks. Inset shows study area that lies in the northern sector of the basement rocks around Masuda in the State of Rajasthan, India.

by Roy, Somani & Sharma (1981). By contrast, the structural geometry in the northern sector is largely unknown, although Sharma & Upadhyay (1975), Sharma (1977), Mukhopadhyay & Dasgupta (1978), Pyne & Bandopadhyay (1985) and Srivastava *et al.* (1995) have studied several aspects of the local geology.

An intensely mylonitized gneiss–migmatite terrane and a relatively undeformed granulite–granitoid terrane are the two main components of the Precambrian basement in the northern sector (Fig. 2). The gneiss–migmatite terrane is a regional-scale shear zone that lies between the Delhi Supergroup rocks on the west and the granulite–granitoid terrane on the east (Fig. 2). This article is concerned with the structural style in the sheared gneiss–migmatite terrane, exposed across an area of 300 km^2 in the western part of the northern sector (Fig. 1). It shows that traditional methods of correlating fold phases are of little value in large-scale ductile shear zones, where successive folds are not only non-cylindrical down to the centimetre-scale, but also identical with respect to geometry and orientation.

3. Mesoscopic structures

3.a. Fold groups and fold sets

The most dominant and regional fabric in the gneiss–migmatite terrane is a mylonite foliation that parallels the contact between different rock types, and traces geometry of the successively developed folds at scales ranging from hand specimen to map (Fig. 2). Mesoscopic-scale folds can be classified into two main fold groups, F_1 and F_2, depending on the lack or presence of deformed lineation, L_1, respectively. L_1 is a group of lineations that parallel the F_1 hinge line, and it consists of intersection/striping lineation and stretching lineation.

Within the F_1 fold group, two fold sets, namely, F_{1A} and F_{1B}, can be distinguished by presence or lack of axial plane foliation, respectively, or by the F_{1A} axial plane folding (Fig. 3a–c). The F_2 fold group is characterized by occurrence of deformed L_1 lineations on the folded surfaces (Fig. 4a). The F_2 fold group also consists of two fold sets, F_{2A} and F_{2B}, that can be distinguished only on those outcrops that display F_{2A} axial plane folding by F_{2B} folds (Fig. 4b). F_1 hinge lines and axial planes are folded by F_{2A} and F_{2B} folds, and such overprinting relationships are preserved at a few outcrops (Fig. 4c).

3.b. Interference patterns

Interference patterns of three kinds can be distinguished in the sheared gneiss–migmatite terrane: (1) a Type 3 pattern (Ramsay, 1967, pp. 531–4) that is developed due to interference between F_{1A} and F_{1B} fold sets of the F_1 fold group (Fig. 3c). In this kind of Type 3 pattern, the early fold F_{1A} is characteristically associated with an axial plane mylonite foliation and the fold surfaces are devoid of any deformed lineation; (2) another kind of Type 3 pattern is developed due to interference between the two fold sets, F_{2A} and F_{2B}, that belong to F_2 fold group (Fig. 4b, c). Both F_{2A} and F_{2B} folds, though devoid of any axial plane foliation, are invariably associated with deformed L_1 lineation in this kind of Type 3 pattern; and (3) a boomerang-shaped Type 2 pattern that formed due to non-coaxial interference between F_1 and F_2 fold groups (Fig. 5a). In Type 2 interference patterns, both F_1 axial planes and F_1 hinge lines are folded by F_2 folds (Fig. 5a–c).

3.c. Sheath folds

Sheath folds of two groups, namely F_1 and F_2, are distinct at the mesoscopic scale. F_1 sheath folds, preserved in domains of insignificant F_2 folding, are characterized by the parallelism between the sheath hinge line and L_1 lineation (Fig. 6a). F_1 sheath folds are also represented by a U-shaped intersection lineation (L_1) on the upright axial plane foliation and the elliptical cross-sections (Fig. 6b). F_2 sheath folds are invariably upright and they characteristically contain deformed L_1 lineations that run oblique or orthogonal to

https://doi.org/10.1017/S0016756810000610 Published online by Cambridge University Press

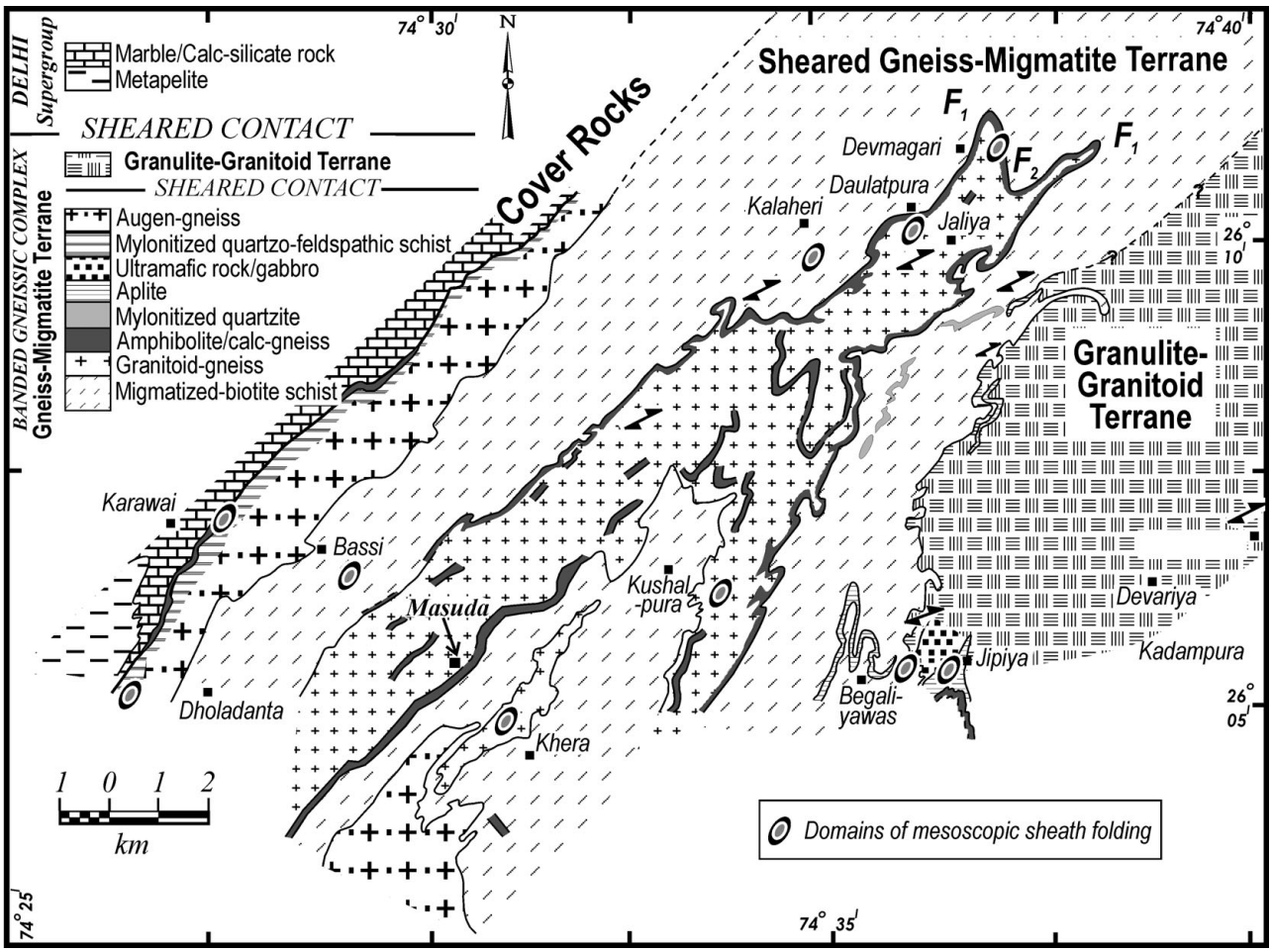

Figure 2. Geological map of a part of the basement rocks that consists of an intensely sheared gneiss–migmatite terrane on the west, and a relatively undeformed granulite–granitoid terrane on the east (after Srivastava, 2001). Contact between the two terranes is ductilely sheared. The gneiss–migmatite terrane is a regional-scale ductile shear zone that lies between the granulite–granitoid terrane and the cover rocks of the Delhi Supergroup.

the sheath hinge line (Fig. 6c, d). Despite the common occurrence of upright F_1 sheath folds, there are a few outcrops where the F_1 sheath fold axial plane dips at a sub-horizontal or low angle (Fig. 6b). The variation in the attitude of the F_1 sheath fold axial plane implies refolding of F_1 sheath folds during F_2 folding.

4. Structural geometry

4.a. Geometry of mesoscopic-scale folds

Observations at the outcrops, where distinction among different fold sets are possible, imply that strongly curvilinear hinge lines and NNE-striking upright axial planes are the common characteristics of all the four fold sets, namely F_{1A}, F_{1B}, F_{2A} and F_{2B}. For the purpose of structural analysis, therefore, F_{1A} and F_{1B} fold sets that characteristically lack deformed L_1 lineations are grouped as F_1 folds. Similarly, F_{2A} and F_{2B} fold sets that contain deformed L_1 lineations on their folded surfaces are grouped as F_2 folds.

The lower hemisphere projections of poles to axial planes and hinge lines of F_1 and F_2 fold groups show identical distribution patterns (Fig. 7a–d). These distribution patterns imply that both F_1 and F_2 group folds are characterized by isoclinal geometry, NNE-striking upright axial planes and strongly curvilinear hinge lines. This interpretation is substantiated by several outcrops where both F_1 and F_2 folds are isoclinal and coplanar except at F_2 hinge zones, where F_1 and F_2 axial planes are characteristically orthogonal to each other (Fig. 5b, c). The orthogonal relationship between F_1 and F_2 axial planes has served as a useful criterion for locating F_2 hinge zones during the structural mapping.

The similarity in F_1 and F_2 hinge line distribution patterns is the effect of two factors (Fig. 7b, d). First, the directional instability in F_1 and F_2 hinge lines was decreased due to their rotation towards the maximum stretching direction (X) during the ductile shearing. Second, the extremely tight and isoclinal nature of F_2 folding resulted in rotation of F_1 axial planes and F_1 limbs into parallelism with F_2 axial planes (Fig. 8). Lower hemisphere projections of strongly curvilinear F_1 and F_2 hinge lines show similar distribution patterns because fold hinge lines lie on their respective axial planes that are approximately parallel to each other (Fig. 7b, d).

https://doi.org/10.1017/S0016756810000610 Published online by Cambridge University Press

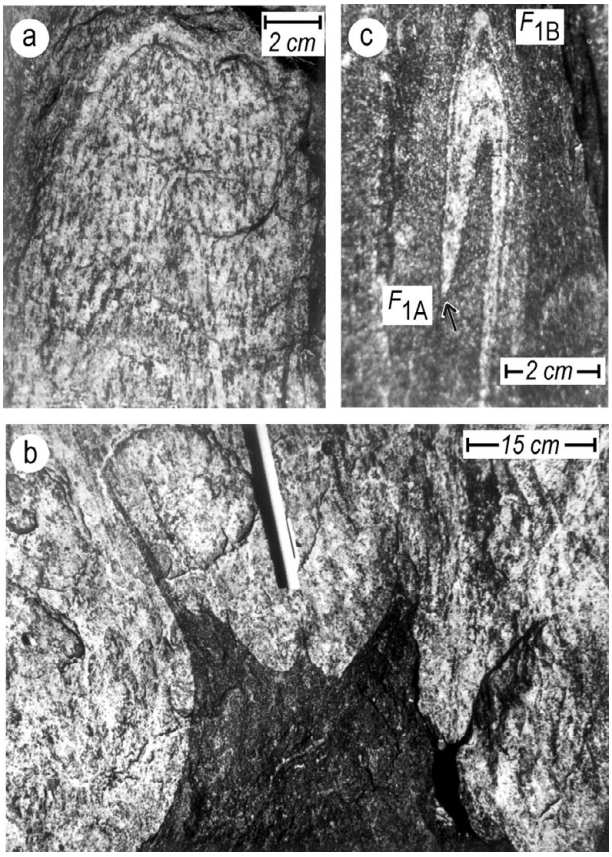

Figure 3. F_1 group folds. (a) The axial plane mylonite foliation characteristically cuts through F_{1A} fold hinge zone in the granite gneiss. (b) Cuspate–lobate F_{1A} folds traced by the contact surface between amphibolite (black) and gneiss (grey). Axial plane mylonite foliation, parallel to pencil, cuts through fold hinge zones. (c) Hook-shaped Type 3 pattern formed due to interference between F_{1A} and F_{1B} folds in the migmatized-biotite schist. F_{1A} and F_{1B} folds are not only isoclinal and coaxial but also coplanar, except at F_{1B} hinge zone. In this kind of Type 3 interference pattern, the F_{1A} hinge zone is associated with axial plane mylonite foliation (indicated by arrow). For a larger version of this figure, see online appendix at http://www.cambridge.org/journals/geo.

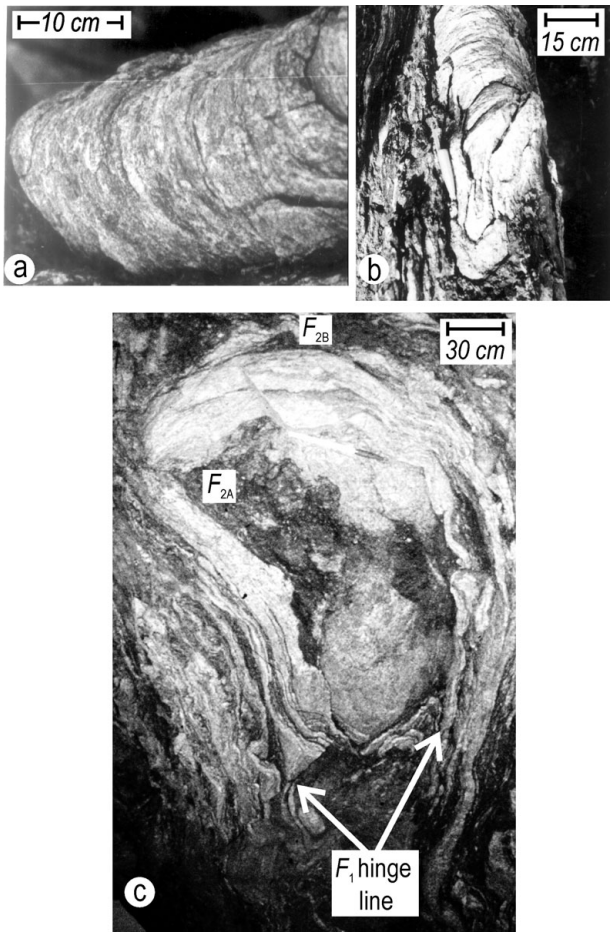

Figure 4. F_2 group folds. (a) Deformed L_1 lineation, defined by intersection/striping lineation and stretching lineation, on F_2 fold hinge zone in the migmatized-biotite schist. (b) Type 3 pattern formed due to interference between F_{2A} and F_{2B} folds in the migmatized-biotite schist. This kind of Type 3 pattern is characterized by the occurrence of deformed L_1 lineation on the fold surfaces. (c) Refolding of F_1 hinge line (indicated by white arrows) and F_1 axial plane by F_{2A} and F_{2B} folds in the granite gneiss. F_{2A} and F_{2B} folds interfere to produce Type 3 pattern. For a larger version of this figure, see online appendix at http://www.cambridge.org/journals/geo.

4.b. Geometry of domain-scale sheath folds

Structural analyses of sheath folds in ten different domains, ranging in scale from a few metres to a few tens of metres, reveal that most F_1 and F_2 sheath folds are characterized by NNE–NE-striking and upright to steeply dipping axial planes, and strongly curvilinear hinge lines (Fig. 9a–j). Lower hemisphere projections of the poles to axial planes and hinge lines of the F_1 and F_2 folds observed at different outcrops (Fig. 7a–d), and those for the F_1 and F_2 sheath folds in different domains (Fig. 9a–j), show identical distribution patterns. The variably plunging F_1 and F_2 folds at different outcrops, therefore, represent different segments of F_1 and F_2 sheath folds, respectively. The presence of two generations of sheath folding, F_1 and F_2, is a common feature in the gneiss–migmatite terrane, and it occurs at scales that are as small as a few square centimetres.

4.c. Geometry of large-scale structure

Contacts between different rock types parallel a mylonite foliation that traces large-scale fold geometry. The mylonite foliation strikes NNE–NE and dips at a very steep angle, except at F_2 hinge zones where its strike swerves to the NNW or NW. The gneiss, the amphibolite, and the migmatized-biotite schist control the map pattern and repeat at different structural levels due to successive folding and sheath folding in the sheared gneiss–migmatite terrane (Fig. 2).

The hinge zone of the large-scale fold is a crescent- or saddle-shaped Type 2 interference pattern, exposed to the northeast of Jaliya (Fig. 2). The sag in the saddle is the large-scale F_2 hinge zone that is flanked by the F_1 antiforms on either side. Vergence of smaller order F_1 and F_2 folds, occurring at limbs of the large-scale fold, is characteristically inconsistent due to superposition of

https://doi.org/10.1017/S0016756810000610 Published online by Cambridge University Press

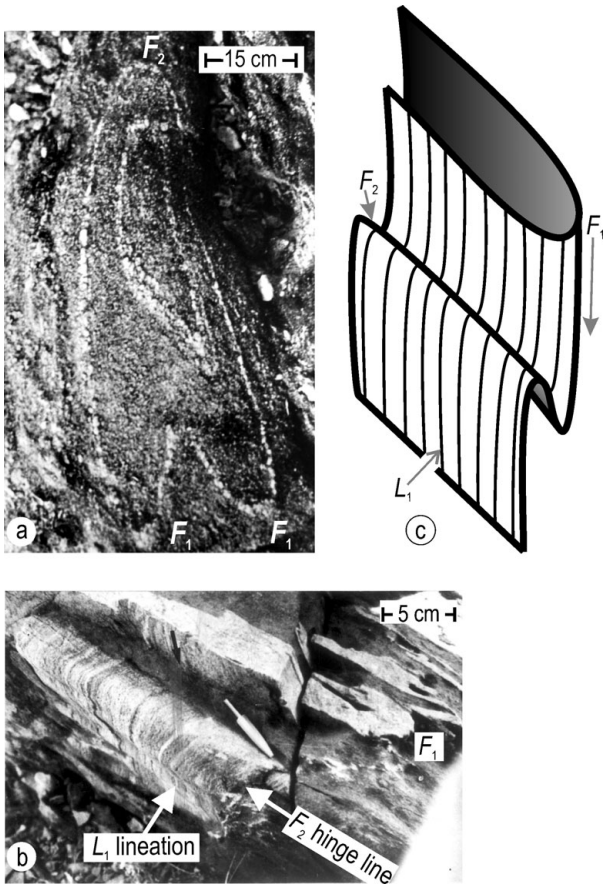

Figure 5. (a) Boomerang-shaped Type 2 pattern formed by interference between F_1 and F_2 folds in the granite gneiss. Both F_1 and F_2 folds are tight to isoclinal and their axial planes are inclined at a low angle to each other. (b, c) Outcrop and sketch of an F_2 fold that refolds F_1 folds in the migmatized-biotite schist. Both F_1 and F_2 folds are isoclinal and coplanar, except at the very small F_2 hinge zone. Intersection lineation (L_1) parallels F_1 hinge line and plunges at subhorizontal and subvertical angles at F_2 hinge zone and limbs, respectively. For a larger version of this figure, see online appendix at http://www.cambridge.org/journals/geo.

S on *Z*, and *Z* on *S* folds, and the inversion in the plunge direction due to sheath folding (Alsop & Holdsworth, 1999).

Despite successive folding, refolding and sheath folding, the synoptic stereoplots for foliation and lineation depict deceptively simple distribution patterns, namely, a point maximum for poles to foliation, and a great circle distribution for lineation (Fig. 10a, b). The point maximum pattern for poles to foliation is primarily due to the isoclinal geometry and an approximate parallelism between the axial planes of successively developed folds. As the axial planes and the limbs of successive folds rotated towards the upright principal plane, *XY*, of the finite strain ellipsoid during progressive ductile shearing (Escher & Watterson, 1974), they assumed an approximately isoclinal geometry and coplanar relationship (Figs 8, 11a, b). Superposition of pure shear on simple shear further brought the axial planes and limbs of successively developed folds closer to each other with respect to the orientation (Fig. 11c). Eventually all the folds assumed extremely tight and isoclinal geometries and coplanar relationships with respect to each other (Fig. 8). The great circle distribution of the hinge lines is also due to rotation of variably oriented hinge lines towards the vertically directed maximum stretching (*X*-axis) during the course of ductile shearing.

A comparison of the distribution patterns of lower hemisphere projections reveals that the geometry of different fold groups at mesoscopic scale and that of the regional-scale fold are identical to geometry of outcrop-scale sheath folds (Figs 7, 9, 10). NNE–NE-striking upright axial planes and strongly curvilinear hinge lines are the common geometrical characteristics of all the folds, irrespective of their relative order and scale of development. The regional-scale folds are, therefore, examples of the interference patterns and the sheath folds that were formed during the course of progressive ductile shearing.

5. Kinematic interpretations

5.a. Elliptical folds

Mesoscopic-scale elliptical folds are common in the sheared gneiss–migmatite terrane (Fig. 12a–e). Three-dimensional exposures reveal that the elliptical outcrop patterns are sections through tight to isoclinal, upright and plane-noncylindrical folds. Three alternative mechanisms could be considered for development of the elliptical folds with curvilinear hinge lines: (1) Type 1 interference between the two fold sets (Ramsay, 1967, pp. 521–5), (2) simultaneous shortening of a layer in different directions during a constrictional deformation (Ramsay & Huber, 1983, p. 66), and (3) sheath folding (Carreras, Estrada & White, 1977; Ramsay, 1980).

That the elliptical folds do not represent a Type 1 interference pattern is apparent from two lines of evidence: (1) lack of two sets of axial planes at high angle to each other and, (2) lack of such arrays of ellipses that contain two sets of axial traces paralleling major and minor axes of successive ellipses (e.g. fig. 10–6 in Ramsay, 1967, p. 525). The alternative mechanism of constrictional deformation is also ruled out because of the consistency in orientation of the axial surface of elliptical folds. The folds developed in a constrictional deformation are typically inconsistent with respect to the axial plane orientation (Ghosh & Ramberg, 1968).

The ubiquity of shear structures such as the mylonite foliation, the *S–C* fabric and the rotated asymmetrical megacrysts implies that the entire gneiss–migmatite terrane is extensively sheared (Fig. 13a). As many folds and interference structures are demonstrably confined within the mesoscopic-scale ductile shear zones, it is evident that these structures were developed during the course of a progressive ductile shearing (Fig. 13b, c). The occurrence of elliptical folds in a setting of intense ductile shearing implies that these structures are the two-dimensional sections of sheath folds.

https://doi.org/10.1017/S0016756810000610 Published online by Cambridge University Press

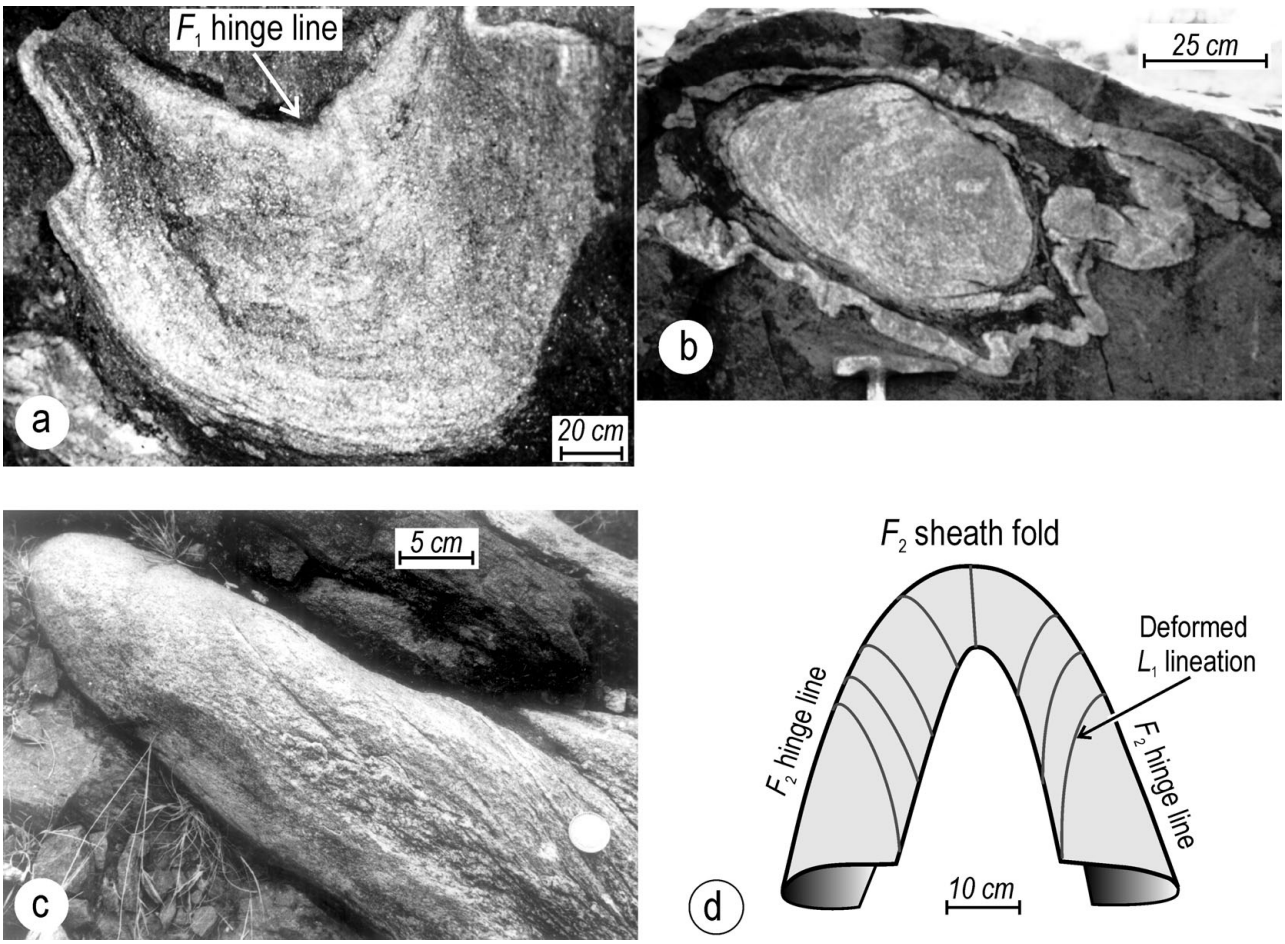

Figure 6. Mesoscopic-scale sheath folds. (a) An extremely tight and isoclinal F_1 sheath fold in granite gneiss. Intersection lineation (L_1), visible on partially eroded surface of the sheath, runs parallel to curvilinear hinge line of the sheath fold. (b) Vertical cross-section of a F_1 sheath fold in the granite gneiss. The sheath fold axial plane dips at a low angle towards the northwest. (c) F_2 sheath fold with deformed stretching lineation L_1 (near the coin) in the granite gneiss. L_1 lineation runs oblique to the sheath fold hinge line. (d) A typical upright and isoclinal F_2 sheath fold in the migmatized-biotite schist (traced from photograph). Intersection lineation (L_1) runs oblique/orthogonal to the sheath fold hinge line, and the unrolled patterns of lineation (L_1) are rectilinear and curvilinear (V-shaped) on apical zone and limbs of the sheath fold, respectively.

The geometry of elliptical folds is an indicator of the type of bulk strain prevalent during the development of sheath folds (Alsop & Holdsworth, 2006). The shapes of elliptical cross-sections, that is, sections normal to the longest axis of the sheath, that develop in simple shear, general shear and constrictional types of bulk strains are characteristically analogous-eye-fold, cats-eye-fold and bulls-eye-fold, respectively (Alsop & Holdsworth, 2006). The axial ratio of the outermost ellipse, a, is equal to, less than, and greater than the axial ratio of the innermost ellipse, b, in the sheath folds that are developed in simple shear, general shear and constrictional strain regimes, respectively (Fig. 14).

Geometrical analyses of ten elliptical cross-sections of the sheath folds reveal that the axial ratio of the outermost ellipse is, in general, less than that of the innermost ellipse (average $R' = 0.71$ in Fig. 14). Furthermore, the thickness of individual layers along the major axis of the ellipse is 2.2 to 9 times greater than the thickness along the minor axis, and the average ratio of thickness along the major and the minor axes is of the order of 4.6. These geometrical characteristics suggest that most elliptical folds are cats-eye-shaped folds that develop in the general shear, that is, a combination of simple shear and pure shear types of bulk strain (Alsop & Holdsworth, 2006).

5.b. Deformed lineations

Intersection or striping lineation L_1, though common in the migmatized-biotite schist, is rare or absent in other rocks. Unrolling of the transparent tracings, laid directly over F_2 folds, yields both curvilinear and rectilinear patterns of deformed L_1 lineations (Srivastava, 2001). Figure 6d illustrates the deformed L_1 lineations over an antiformal upright and isoclinal F_2 sheath fold in the migmatized-biotite schist. The unrolled patterns of deformed L_1 lineation are characteristically rectilinear and V-shaped on the apical zone and the limbs of the sheath fold, respectively. It is noteworthy

https://doi.org/10.1017/S0016756810000610 Published online by Cambridge University Press

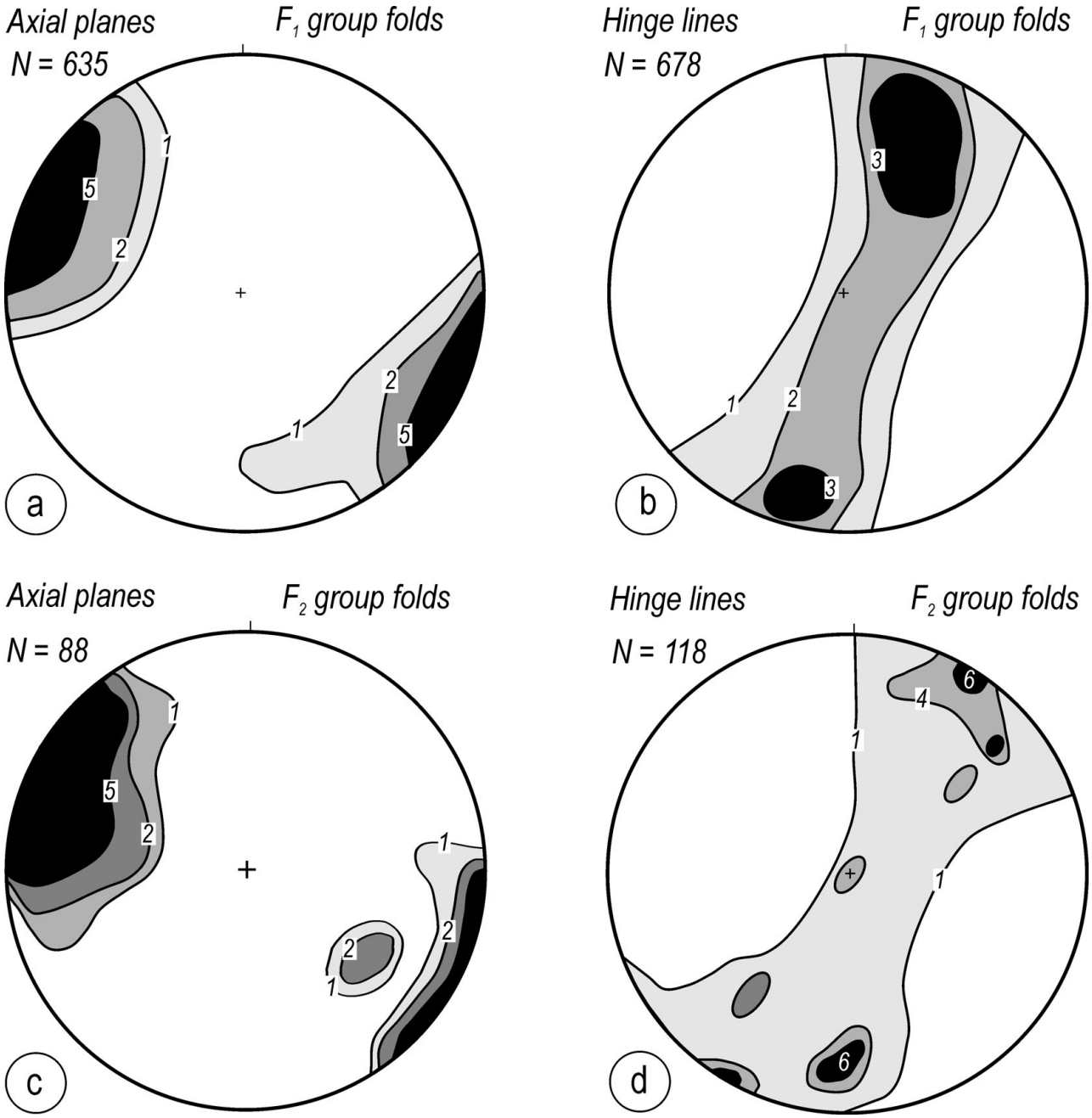

Figure 7. (a–d) Lower hemisphere, equal area projections of poles to axial planes and hinge lines of mesoscopic-scale F_1 and F_2 folds that occur as isolated folds at different outcrops. Contours: % per 1 % area.

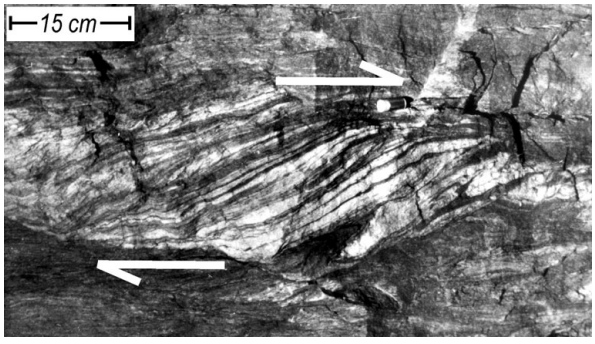

Figure 8. A series of coaxially refolded folds within a dextral ductile shear zone in the granite gneiss. The folds are so tight and isoclinal that their axial planes parallel each other.

that most V-patterns are symmetrical about the F_2 hinge line, and the V-patterns become progressively tighter with increase in the plunge angle of the F_2 hinge line.

Based on the theoretical modelling and the natural examples of deformed lineations from the Phulad area, which lies close to the study area in this article, Ghosh, Hazra & Sengupta (1999) showed that the rectilinear pattern develops when the fold hinge lines are initiated subparallel to the intermediate axis of the strain ellipsoid, whereas the symmetrical V-patterns form when the fold hinge line and lineation are orthogonal and the bulk strain is of general shear type. The common occurrence of the symmetrical V-shaped

https://doi.org/10.1017/S0016756810000610 Published online by Cambridge University Press

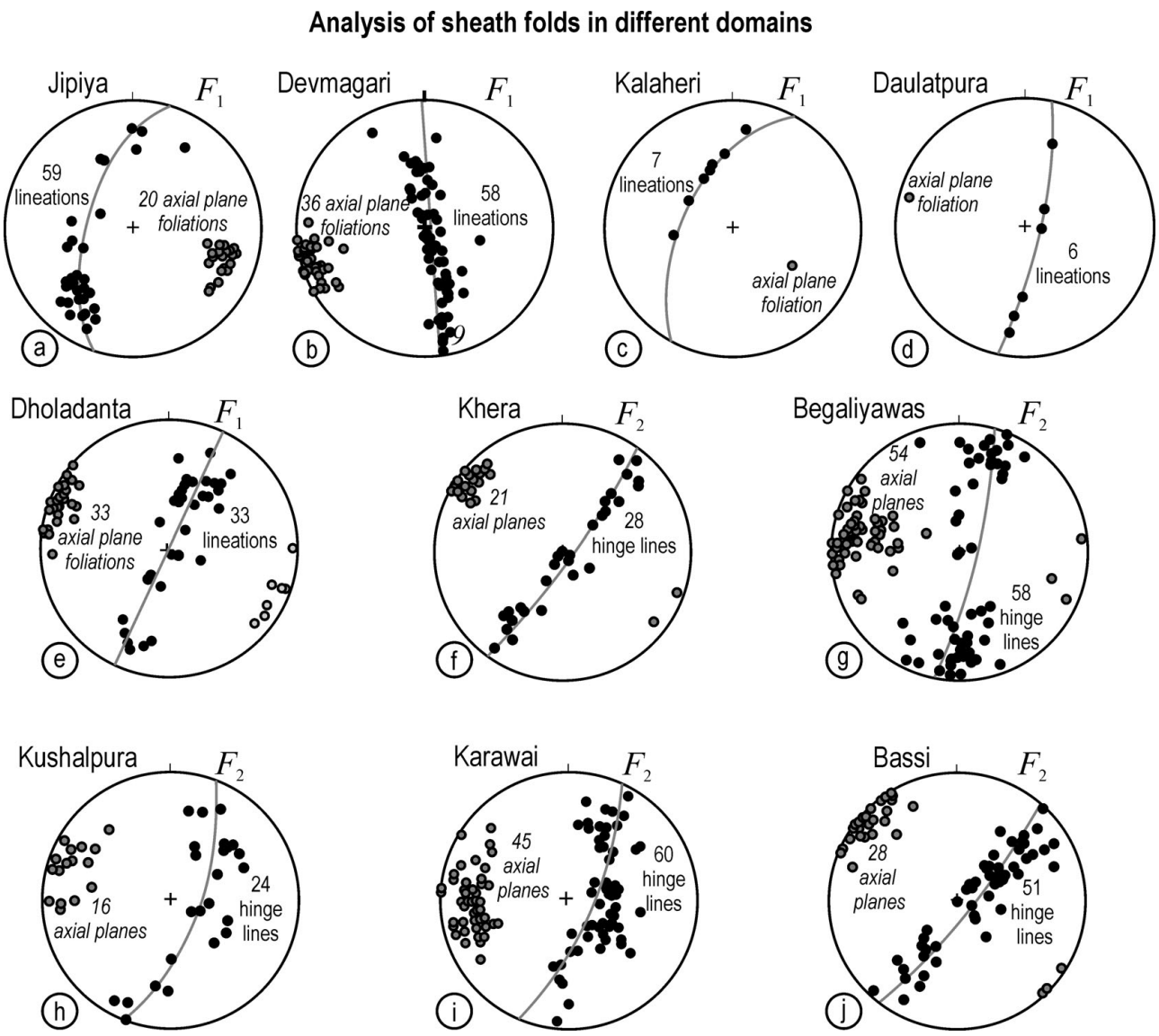

Figure 9. Lower hemisphere, equal area projections of poles to axial planes and hinge lines/intersection lineation of sheath folds in different domains (after Srivastava, 2001). (a–e) F_1 sheath folds. Intersection lineation parallels F_1 hinge line and lies on the F_1 sheath fold axial plane. (f–j) F_2 sheath folds. F_1 and F_2 sheath folds are approximately identical with respect to geometry and orientation. Location of outcrop/village mentioned on each stereogram is shown in Figure 2.

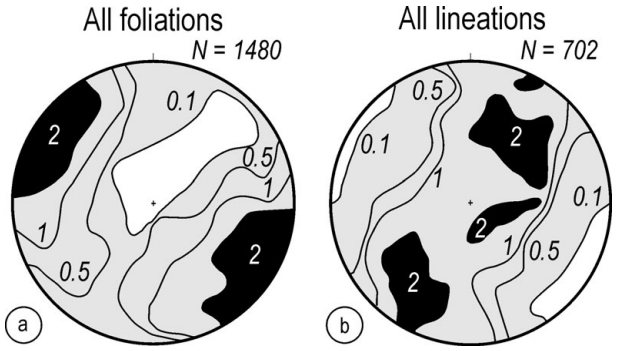

Figure 10. (a, b) Synoptic plots show lower hemisphere, equal area projections of poles to mylonite foliation and hinge line parallel lineations in the entire gneiss–migmatite terrane (after Srivastava, 2001). N: number of observations. Contours: 0.05–0.5–1–2 % and 0.1–0.5–1–2 % per 1 % of the area in (a) and (b), respectively.

deformed lineation pattern in the study area, therefore, implies that the F_2 hinge lines were initiated at right angles to the dominant orientation of F_1 hinge lines, at least in some domains, and F_2 sheath folds were developed in a general shear type of bulk strain.

6. Summary and conclusions

Two major fold groups, F_1 and F_2, each containing at least two coaxial fold sets, were developed during progressive ductile shearing in the gneiss–migmatite terrane (Fig. 15a, b). As the fold sets that belong to the same fold group were initiated on a commonly directed hinge line, their interference produced a characteristic Type 3 pattern. By contrast, the non-coaxial refolding of F_1 group folds by F_2 group folds resulted in the development of Type 2 interference pattern at scales

https://doi.org/10.1017/S0016756810000610 Published online by Cambridge University Press

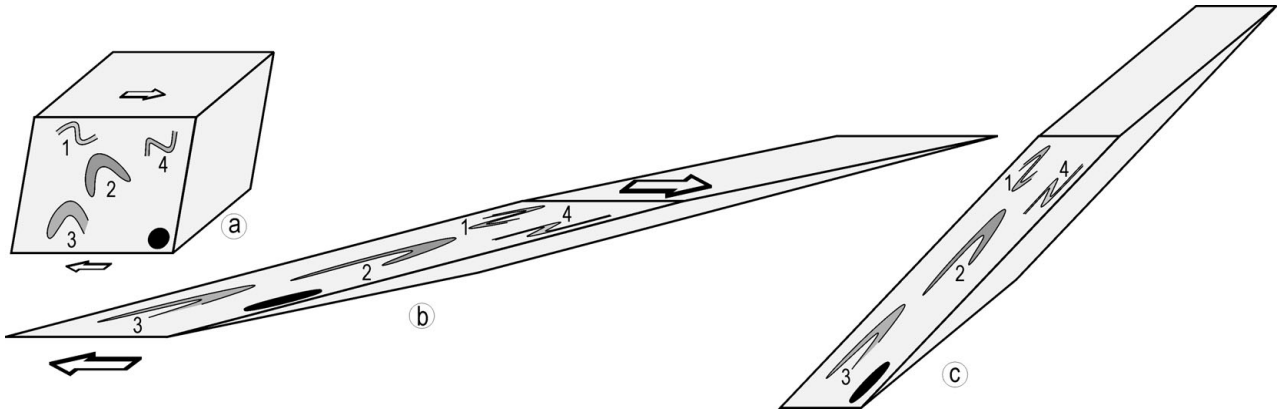

Figure 11. Schematic diagrams show geometrical modification of structures during the ductile shearing in a general shear type of deformation regime. (a, b) Simple shear. (c) Pure shear. (a) Ductile shear zone contains folds (1 and 4), Type 2 interference pattern (2) and Type 3 interference pattern (3). The axial planes of different folds are at high angle to each other at this stage. Black ellipse: strain ellipse. (b) At advanced stage of shearing, say $\gamma = 3.73$, variably oriented fold axial planes rotate towards the principal plane (*XY*) of the strain ellipsoid (black). As a sequel to this rotation, all the folds and interference patterns become very tight or isoclinal, and approximately coplanar. (c) Superposition of pure shear (strain ratio = 4.0) on simple shear in (b) further tightens the folds and the interference patterns, and enhances the parallelism between fold axial planes and limbs due to their rotation towards *XY* plane of the strain ellipsoid.

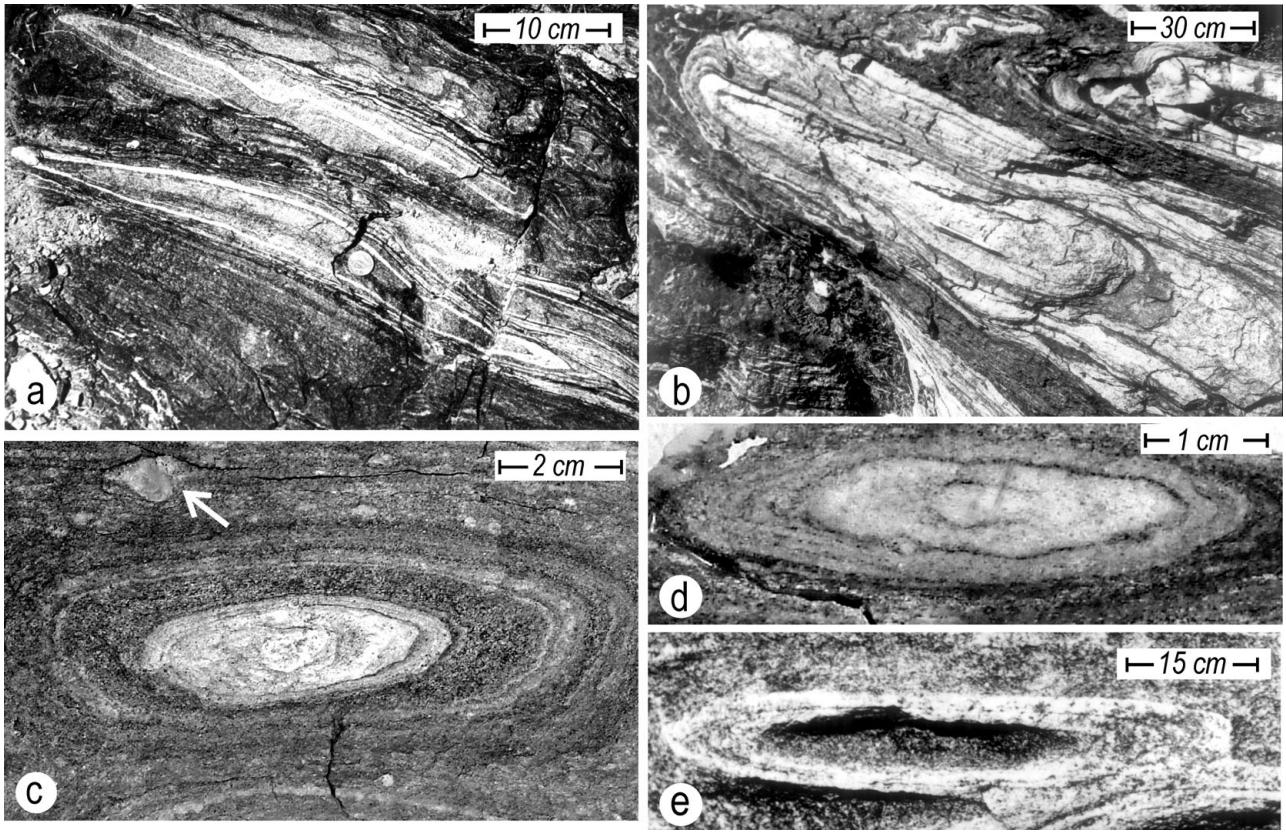

Figure 12. Elliptical outcrop patterns exposed on sections normal to the longest axes of sheath folds. Approximately isoclinal nature and the cats-eye geometry of elliptical folds are noteworthy. (a, b, e) Granite gneiss; (c, d) migmatized-biotite schist. White arrow in (c) points to a σ-shaped quartz megacryst in the mylonite.

ranging from outcrop to map (Fig. 15c). Progressive ductile shearing modified both F_1 and F_2 group folds into sheath folds. Several lines of evidence, such as the variation in attitude of F_1 sheath axial planes and the occurrence of deformed intersection lineation on F_2 sheath folds point to two successive phases of sheath folding during the progressive shearing in the gneiss–migmatite terrane.

https://doi.org/10.1017/S0016756810000610 Published online by Cambridge University Press

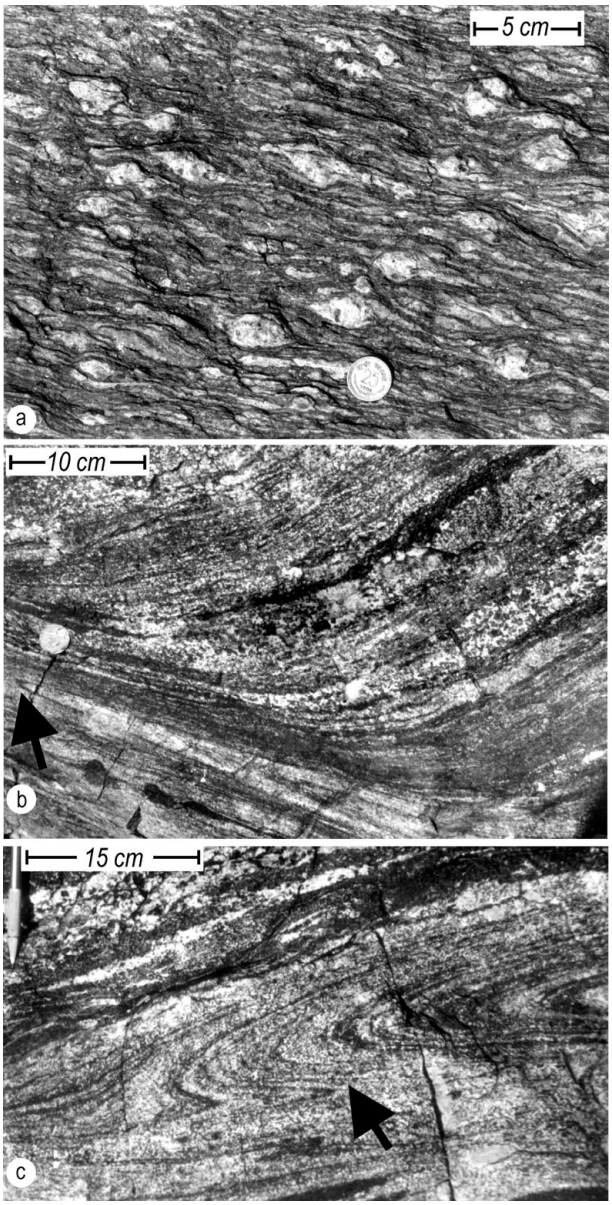

Figure 13. (a) σ-shaped asymmetrical megacrysts in the granite gneiss mylonite. (b) Occurrence of an isoclinal fold (indicated by arrow) within a dextral ductile shear zone in the granite gneiss. (c) Type 3 interference pattern confined within a ductile shear zone in the granite gneiss. Arrow points to the hinge zone of early fold in the interference pattern.

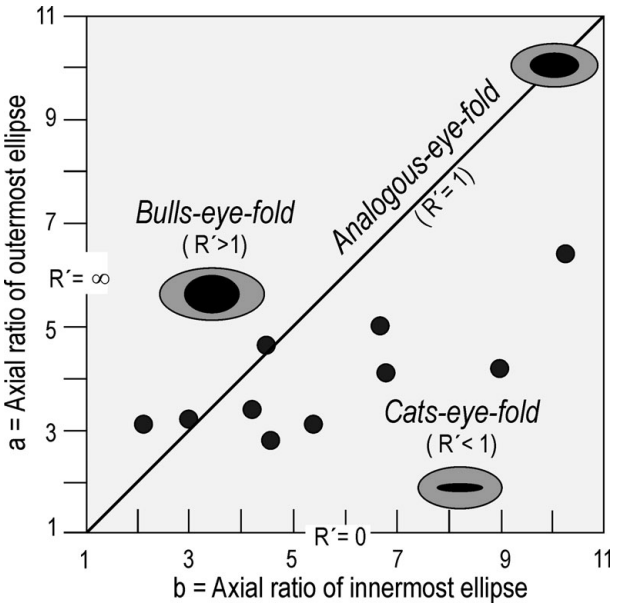

Figure 14. Cartesian plot for shape representation of elliptical folds and determination of nature of bulk strain (after Alsop & Holdsworth, 2006). Cats-eye shape of most elliptical folds suggests a general shear type of bulk strain. $R' = a/b$, where a and b are axial ratios of the outermost and the innermost ellipses, respectively, in an elliptical fold.

This study proposes that a very large amount of rotation of axial planes and hinge lines during a progressive ductile shearing can impart identical styles to successively developed folds. In a ductile shear zone, successive folds initiate on curvilinear hinge lines because the mylonite foliation that traces these folds is inherently curviplanar (Ghosh, Hazra & Sengupta, 1999). During the progressive ductile shearing, the hinge lines of successive folds become strongly curved, and their limbs and the axial planes assume a near parallelism due to their rotation towards the XY principal plane of the bulk strain ellipsoid (Fig. 11a, b). At a moderate or high magnitude of shear strain, say $\gamma = 3.73$, all the folds and the interference patterns, irrespective of their order of development, become extremely tight to isoclinal, strongly noncylindrical and approximately coplanar, except in the very short hinge zones of the late folds (Fig. 11b). The superposition of pure shear on simple shear further tightens the folds and helps achieve the coplanar relationship between successively developed folds (Fig. 11c). It is due to these modifications in fold geometry that several generations of successively developed folds are not only isoclinal, but also approximately coplanar in the intensely sheared gneiss–migmatite terrane.

Several lines of evidence, such as the cats-eye shape of elliptical folds and the symmetrical V-shapes of deformed lineations, imply that ductile shearing occurred in a general shear, that is, simple shear and pure shear, type of bulk strain regime. The occurrence of symmetrical V-shapes of deformed lineations and the orientation of fabric elements further imply that a very large amount of subvertically directed stretching occurred due to intense NNW–SSE-directed horizontal compression in the gneiss–migmatite terrane (Ghosh, Hazra & Sengupta, 1999).

Acknowledgements. I am grateful to Ian Alsop and an anonymous referee for erudite reviews and constructive suggestions. I also thank my students, in particular, Akshay Pradhan, Sanjoy Nag, Jayram Sahoo and Abhijit Bordoloi, who helped map the basement rocks during different phases of the project. Prof. V. Rajamani (JNU) encouraged me to study the basement rocks in Rajasthan. This work was supported by the 'Deep Continental Studies' Program of the Department of Science and Technology, Government of India.

https://doi.org/10.1017/S0016756810000610 Published online by Cambridge University Press

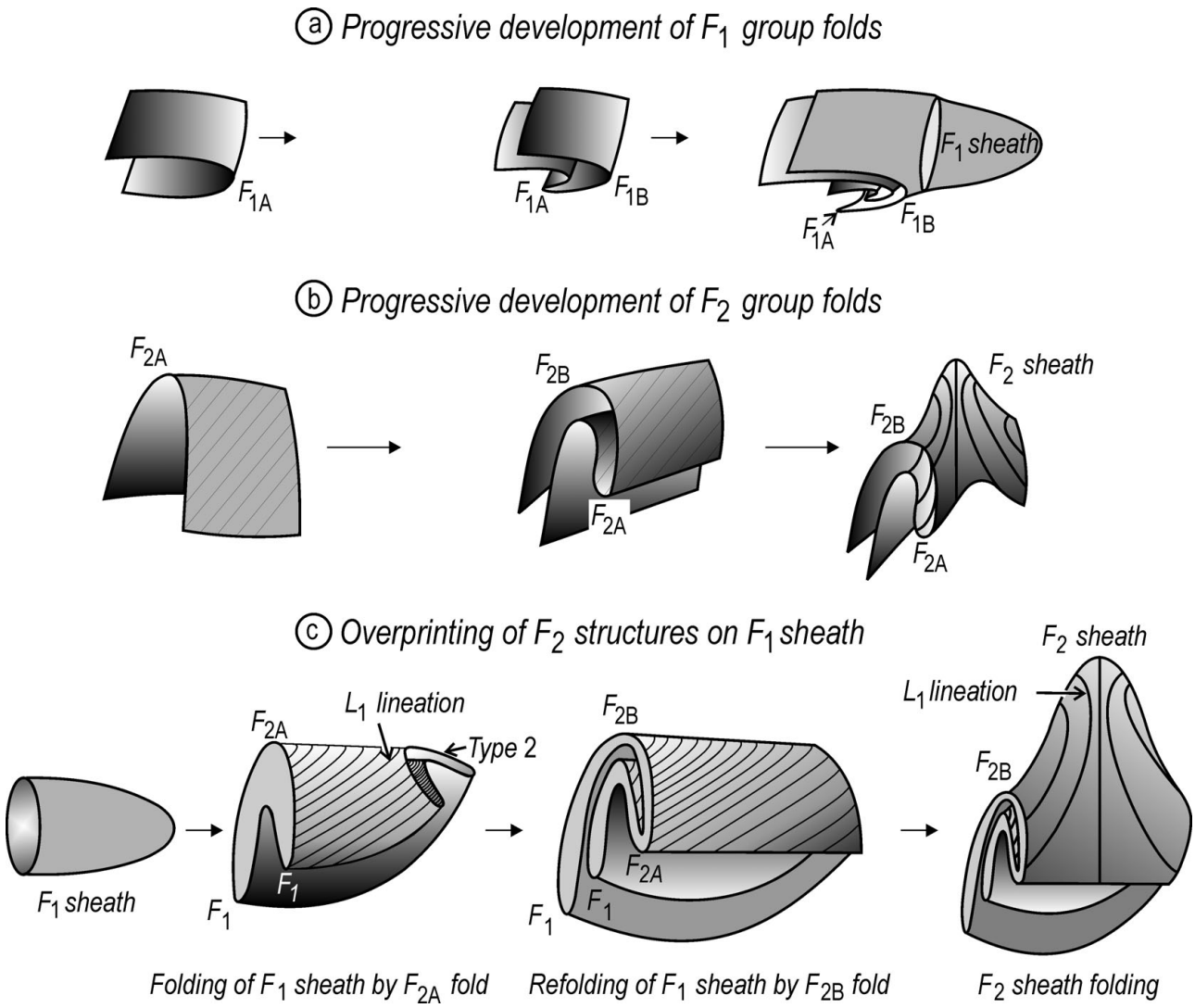

Figure 15. Schematic diagrams show the geometrical evolution of F_1 and F_2 group folds and successive sheath folds during progressive shearing. (a) F_1 group folds show coaxial refolding and F_1 sheath folding. (b) F_2 group folds show coaxial refolding and F_2 sheath folding. (c) Progressive folding and refolding of an F_1 sheath by F_{2A} and F_{2B} folds, and F_2 sheath folding.

References

ALSOP, G. I. & CARRERAS, J. 2007. The structural evolution of sheath folds: a case study from Cap de Creus. *Journal of Structural Geology* **29**, 1915–30.

ALSOP, G. I. & HOLDSWORTH, R. E. 1999. Vergence and facing patterns in large-scale sheath folds. *Journal of Structural Geology* **21**, 1335–49.

ALSOP, G. I. & HOLDSWORTH, R. E. 2004*a*. The geometry and topology of natural sheath folds: a new tool for structural analysis. *Journal of Structural Geology* **26**, 1561–89.

ALSOP, G. I. & HOLDSWORTH, R. E. 2004*b*. Shear zone folds: records of flow perturbation or structural inheritance? In *Flow Processes in Faults and Shear Zones* (eds G. I. Alsop, R. E. Holdsworth, K. J. W. McCaffrey & M. Hand), pp. 177–99. Geological Society of London, Special Publication no. 224.

ALSOP, G. I. & HOLDSWORTH, R. E. 2006. Sheath folds as discriminators of bulk strain type. *Journal of Structural Geology* **28**, 1588–606.

ALSOP, G. I. & HOLDSWORTH, R. E. 2007. Flow perturbation folding in shear zones. In *Deformation of the Continental Crust: The Legacy of Mike Coward* (eds A. C. Ries, R. W. H. Butler & R. D. Graham), pp. 77–103. Geological Society of London, Special Publication no. 272.

ALSOP, G. I., HOLDSWORTH, R. E. & MCCAFFREY, K. J. W. 2007. Scale invariant sheath folds in salt, sediments and shear zones. *Journal of Structural Geology* **29**, 1585–604.

CARRERAS, J., ESTRADA, A. & WHITE, S. 1977. The effects of folding on c-axis fabric of quartz mylonite. *Tectonophysics* **39**, 3–24.

COBBOLD, P. R. & QUINQUIS, H. 1980. Development of sheath folds in shear regimes. *Journal of Structural Geology* **2**, 119–26.

ESCHER, A. & WATTERSON, J. 1974. Stretching fabrics, folds and crustal shortening. *Tectonophysics* **22**, 223–31.

FAURE, M. 1985. Microtectonic evidence for eastward ductile shear in the Jurassic orogen of SW Japan. *Journal of Structural Geology* **7**, 175–86.

FOWLER, A. & KALIOUBI, E. 2002. The migif-Hafafit gneissic complex of the Egyptian desert: fold interference patterns involving multiply deformed sheath folds. *Tectonophysics* **346**, 247–75.

GHOSH, S. K. & RAMBERG, H. 1968. Buckling experiments on intersecting fold patterns. *Tectonophysics* **5**, 89–105.

https://doi.org/10.1017/S0016756810000610 Published online by Cambridge University Press

GHOSH, S. K. & SENGUPTA, S. 1987. Progressive evolution of structures in a ductile shear zone. *Journal of Structural Geology* **9**, 277–87.

GHOSH, S. K., HAZRA, S. & SENGUPTA, S. 1999. Planar, non-planar and refolded sheath folds in the Phulad shear zone, Rajasthan, India. *Journal of Structural Geology* **21**, 1715–29.

GOSCOMBE, B. 1991. Intense non-coaxial shear and the development of mega-scale sheath folds in the Arunta Block, Central Australia. *Journal of Structural Geology* **13**, 299–318.

HENDERSON, J. R. 1981. Structural analysis of sheath folds with horizontal *X*-axes, northeast Canada. *Journal of Structural Geology* **3**, 203–10.

HERON, A. M. 1953. The geology of central Rajputana. *Geological Survey of India Memoir* **79**, 389 pp.

HOLDSWORTH, R. E. 1990. Progressive deformation structures associated with ductile thrusts in the Moine Nappe, Sutherland, N. Scotland. *Journal of Structural Geology* **12**, 443–52.

LACASSIN, R. & MATTAUER, M. 1985. Kilometre-scale sheath fold at Mattmark and implications for transport direction in the Alps. *Nature* **315**, 739–42.

MARQUES, F. O., GUERREIRO, S. M. & FERNANDES, A. R. 2008. Sheath fold development with viscosity contrast: analogue experiments in bulk simple shear. *Journal of Structural Geology* **30**, 1348–53.

MAWER, C. K. & WILLIAMS, P. F. 1991. Progressive refolding and foliation development in a sheared, coticule-bearing phyllite. *Journal of Structural Geology* **13**, 539–55.

MIES, W. 1993. Structural-analysis of sheath folds in the Sylacauga-marble-Group, Talladega slate belt, southern Appalachians. *Journal of Structural Geology* **15**, 983–93.

MINNIGH, L. D. 1979. Structural analysis of sheath folds in a meta-chert from the Western Italian Alps. *Journal of Structural Geology* **1**, 275–88.

MUKHOPADHYAY, D. K., BHADRA, B. K., GHOSH, T. K. & SRIVASTAVA, D. C. 1997. Development of compressional and extensional structures during progressive ductile shearing in the Main Central Thrust, Lesser Himachal Himalaya. In *Evolution of Geological Structures in Micro- to Macro-Scales* (ed. S. Sengupta), pp. 203–17. London: Chapman and Hall Press.

MUKHOPADHYAY, D. & DASGUPTA, S. 1978. Delhi-pre-Delhi relations near Badnor. *Indian Journal of Earth Sciences* **5**, 183–90.

NAHA, K. & MOHANTY, S. P. 1990. Structural studies in the pre-Vindhyan rocks of Rajasthan: a summary of work of the last three decades. *Proceedings Indian Academy of Sciences* **99**, 279–90.

PLATT, J. P. 1983. Progressive refolding in ductile shear zones. *Journal of Structural Geology* **5**, 619–22.

PYNE, T. K. & BANDOPADHYAY, A. 1985. Structure of Banded Gneissic Complex at and around Bandanwara, Ajmer district, Rajasthan. *Indian Journal of Earth Science* **12**, 9–20.

QUINQUIS, H., AUDREN, C., BRUN, J. P. & COBBOLD, P. R. 1978. Intense progressive shear in Ile de Grouix blueschists and compatibility with subduction or obduction. *Nature* **274**, 43–5.

RAMSAY, J. G. 1967. *Folding and Fracturing of Rocks*. New York: McGraw Hill, 568 pp.

RAMSAY, J. G. 1980. Shear zone geometry, a review. *Journal of Structural Geology* **2**, 83–99.

RAMSAY, J. G. & HUBER, M. I. 1983. *The Techniques of Modern Structural Geology. Vol. 1: Strain Analysis*. London: Academic Press, pp. 1–308.

RAMSAY, J. G. & HUBER, M. I. 1987. *The Techniques of Modern Structural Geology. Vol. 2: Folds and Fractures*. London: Academic Press, pp. 309–700.

RHODES, S. & GAYER, R. A. 1977. Non-cylindrical folds, linear structures in the X direction and mylonite development during translation of the Caledonian Kalak nappe Complex of Finnmark. *Geological Magazine* **115**, 329–41.

ROY, A. B., SOMANI, M. K. & SHARMA, N. K. 1981. Aravalli-pre-Aravalli relationship: a study from the Bhindar region, southern Rajasthan. *Indian Journal of Earth Sciences* **8**, 119–30.

SEARLE, M. P. & ALSOP, G. I. 2007. Eye-to-eye with a mega-sheath fold: a case study from Wadi Mayh, northern Oman Mountains. *Geology* **35**, 1043–6.

SHARMA, R. S. 1977. Deformation and crystallization history of the Precambrian rocks in north central Rajasthan, India. *Precambrian Research* **4**, 133–62.

SHARMA, R. S. & UPADHYAY, T. P. 1975. Multiple deformation in the Precambrian rocks to the southeast of Ajmer, Rajasthan, India. *Journal of the Geological Society of India* **16**, 428–40.

SINHA-ROY, S., MALHOTRA, G. & MOHANTY, M. 1998. *Geology of Rajasthan*. Bangalore: Geological Society of India, 278 pp.

SRIVASTAVA, D. C. 2001. Deformation pattern in the Precambrian basement around Masuda, central Rajasthan. *Journal of the Geological Society of India* **57**, 197–222.

SRIVASTAVA, D. C., YADAV, A. K., NAG, S. & PRADHAN, A. K. 1995. Deformation style of the Banded Gneissic Complex in Rajasthan: a critical evaluation. In *Continental Crust of Northwestern and Central India* (eds S. Sinha-Roy & K. R. Gupta), pp. 199–216. Geological Society of India Memoir no. 31.

TURNER, F. J. & WEISS, L. E. 1963. *Structural Analysis of Metamorphic Tectonites*. McGraw Hill, 545 pp.

https://doi.org/10.1017/S0016756810000610 Published online by Cambridge University Press